Indian Journal of Fibre & Textile Research
Vol. 50, September 2025, pp. 303-309
DOI: 10.56042/ijftr.v50i3.10823

Dyeing and antibacterial properties of silk fabric based on silver nanoparticles

Walaikorn Nitayaphat[1,a] & Thanut Jintakosol[2]

[1]Department of Chemistry, Faculty of Science, Srinakharinwirot University, Bangkok 101 10, Thailand

[2]Gems and Jewellery Program, College of Creative Industry, Srinakharinwirot University, Bangkok 101 10, Thailand

Received 1 May 2024; revised received and accepted 24 October 2024

This study investigates the colouration and antibacterial functionalisation of silk fabrics using silver nanoparticles (AgNPs). The variation in AgNP morphologies imparted a range of colours to the silk, attributed to differences in the nanoparticles' localised surface plasmon resonance. The dyed fabrics are characterised for surface morphology, colour strength, and physical and mechanical properties. Transmission electron microscopy (TEM) analysis reveals that the synthesised AgNPs range in size from 2.8 to 79.8 nm. The resulting fabrics exhibit vivid colours corresponding to the morphological variations of AgNPs deposited on their surfaces. Moreover, the AgNP-dyed silk shows strong antibacterial activity against *Staphylococcus aureus* and *Escherichia coli*. Cationic pretreatment of silk significantly enhances washing fastness. This study demonstrates that AgNP-based dyeing can be effectively performed at room temperature within a short time, offering a low-energy approach to functionalising silk fabrics.

Keywords: Antibacterial, Dyeing, Localised surface plasmon resonance, Silver nanoparticle, Silk

1 Introduction

Textile dyeing involves the uniform application of colourants to a substrate in a solution medium, typically through processes such as dyeing, printing, and pigmenting[1]. In recent years, there has been a growing interest in the functionalisation of textiles to impart additional properties beyond colouration, driven by the expanding applications of multifunctional fabrics. Various active materials, including electrically conductive substances, carbon nanotubes, silica coatings, UV-blocking agents, and metal nanoparticles, have been employed to modify fibre surfaces and achieve functionalities such as flame retardancy[2,3], antibacterial activity[4-6], UV protection[7,8], and self-cleaning capabilities[9,10]. Among these, silver nanoparticles (AgNPs) have received significant attention due to their strong antibacterial properties and ability to produce vivid colours on textiles[11-14]. AgNPs adhere to fibres primarily through electrostatic interactions and impart bright colouration as a result of their localised surface plasmon resonance (LSPR), a collective oscillation of conduction electrons excited by incident light[15,16]. This phenomenon results in pronounced absorption and scattering, observed as distinct peaks in the extinction spectrum. The LSPR characteristics of AgNPs are highly dependent on particle size and shape,[17,18] and recent advances in synthesis techniques have enabled precise control over these parameters, allowing for tunable optical properties and colour output[19-22].

Silk, a natural protein fibre, is extensively utilised in the textile industry due to its soft lustre, luxurious appeal, exceptional comfort, inherent elegant sheen, and environmental sustainability. Enhancing the functional properties of silk through nanoparticle modification has gained considerable attention. For instance, the multifunctionality of silk fibroin fabric was achieved by depositing CeO_2 nanoparticles onto its surface via a dip-coating method, imparting both UV-shielding and antibacterial capabilities[23]. ZnO nanoparticles have been coated on the surface of silk to improve the mechanical and antibacterial properties[24]. In addition, silk fabrics were coloured red and brown with antimicrobial properties by the gold nanoparticles[25,26].

This study investigates the dyeing of silk fabrics using assemblies of silver nanoparticles (AgNPs) that exhibit distinct localised surface plasmon resonance (LSPR) bands. Before dyeing, the silk fabrics are pretreated with a cationic reagent to enhance washing fastness and promote effective binding with anionically charged AgNPs. The colouration of the silk is controlled by tuning the morphology of the AgNPs. The dyeing performance and antibacterial

[a]Corresponding author.
E-mail: walaikorn@g.swu.ac.th

properties of the AgNP-treated silk fabrics are systematically evaluated. Colour strength (K/S) measurements and UV–Vis spectroscopy are employed to characterise the colour and optical properties of the dyed fabrics. The microstructures of the AgNPs and treated silk surfaces are examined using transmission electron microscopy (TEM) and scanning electron microscopy (SEM), respectively. Antibacterial efficacy is assessed against *Staphylococcus aureus* and *Escherichia coli*. This one-step process effectively imparts both vibrant colouration and durable antibacterial functionality to silk fabrics.

2 Materials and Methods

2.1 Materials

Woven silk fabrics (73 g/m^2) purchased from a local fabric store were degummed using a sodium carbonate solution. Silver nitrate ($AgNO_3$) (>99 %), trisodium citrate (≥99.0 %), sodium borohydride (>98.5 %), sodium chloride (>99 %), acetic acid (≥99 %), hydrogen peroxide (30 wt %), and polyvinylpyrrolidone (PVP) (M_w = 40000 gmol^{-1}) and N-(3-chloro-2-hydroxypropyl) trimethylammonium chloride (CHTAC), a cationic reagent, were purchased from Sigma-Aldrich. All chemicals were of analytical-grade.

2.2 Instruments and Measurements

The formation of silver nanoparticles (AgNPs) was visually confirmed by a colour change of the solution from blue to yellow upon adding sodium borohydride ($NaBH_4$). The AgNP solutions were characterised using various techniques. The samples' UV-Visible (UV-vis) absorption spectra were recorded using the UV-2450 spectrophotometer (Shimadzu UV-2450, Japan). Transmission electron microscopy (TEM) was performed using a Philips Tecnai 20 microscope operated at 120 kV to determine nanoparticle morphology and size distribution. The surface morphology of dyed silk fabrics was examined by field-emission scanning electron microscopy (FE-SEM) using a JSM-7610F instrument. The colour strength (K/S value) of AgNP-dyed silk fabrics was measured using a HunterLab UltraScan VIS spectrophotometer. Tensile strength was evaluated using an M100-1CT Testometric Universal Testing Machine according to ASTM D5035–95 (strip method) for the determination of breaking force and elongation. Each reported value represented the mean of at least five individual measurements.

2.3 Preparation of AgNPs

AgNPs exhibiting different colours were synthesised following the method described by Métraux and Mirkin[27]. An aqueous solution of $AgNO_3$ (0.1 mM, 25 mL) was mixed with trisodium citrate (0.1 M, 0.45 mL), hydrogen peroxide (30 wt%, 0.06 mL), and PVP (0.03 g) under vigorous stirring at 30 °C for 30 min. Subsequently, $NaBH_4$ solution (0.1 M) was rapidly added to the mixture in varying volumes (6.0, 8.0, 12.8, 16.0, 16.8, or 20.0% of the $AgNO_3$ solution). After approximately 30 min, AgNPs solutions of varying colours were obtained, corresponding to the amount of $NaBH_4$ employed (Fig. 1).

2.4 Cationic Pretreatment of Silk Fabrics

Silk fabrics were pretreated with CHTAC using a wet chemical process. The treatment was carried out at a reagent concentration of 4 g/L and a liquor ratio of 1:30. The pH was adjusted to 8.0 using NaOH, and the treatment was conducted at 80 °C for 30 min. Following treatment, the fabrics were thoroughly rinsed with deionised water and air-dried at room temperature.

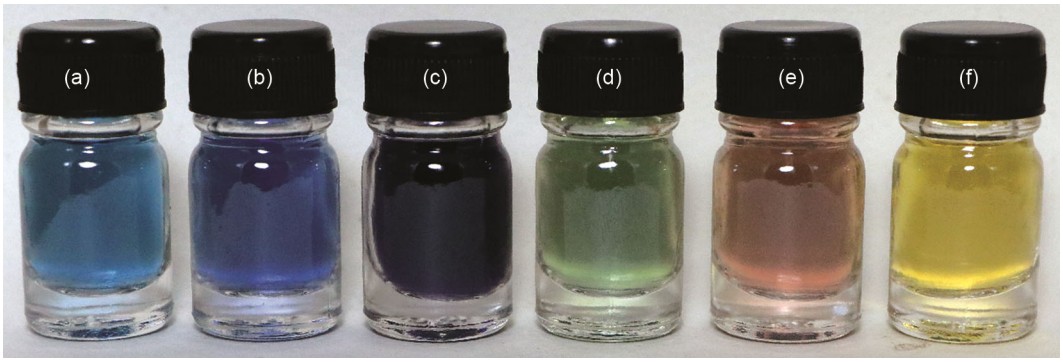

Fig. 1 — Colour variation of synthesised AgNP solutions with increasing 0.1 M $NaBH_4$ concentration: (a) 6.0, (b) 8.0, (c) 12.8, (d) 16.0, (e) 16.8 and (f) 20.0 % by volume of $AgNO_3$ solution

2.5 Dyeing of Silk Fabrics by AgNPs

Silk fabrics were dyed with AgNPs using the exhaustion method. The pH of the AgNP solution was adjusted to 4.0 with acetic acid. The silk fabrics were immersed in the dye bath at a liquor ratio of 1:30 and dyed at 30 °C for 15 min under continuous stirring. After dyeing, the fabrics were rinsed thoroughly with deionised water to remove unbound nanoparticles and dried at room temperature.

2.6 Colour Measurement

The colour parameters of undyed and AgNP-dyed silk fabrics were determined using a HunterLab UltraScan VIS spectrophotometer under D65 illumination and a 10° standard observer. Measurements were taken at three different positions on each sample, and the average values were reported. The CIE L*a*b* colour space parameters were recorded, where L* represents brightness, a* denotes the red-green axis (+ values indicate red, – values indicate green), and b* corresponds to the yellow-blue axis (+ values indicate yellow, – values indicate blue). Additionally, the colour strength (K/S) values were measured to evaluate dye uptake.

The total colour difference (ΔE) between the undyed and dyed fabrics was calculated using the following equation[28,29]:

$$\Delta E = [(L_0^*-L)^2 + (a_0^*-a)^2 + (b_0^*-b)^2)]^{1/2} \quad \ldots (1)$$

where L_0^*, a_0^*, and b_0^* are the colour coordinates of the undyed fabrics; and L*, a*, and b* are those of the dyed fabric.

2.7 Evaluation of the Antibacterial Activity

The antibacterial activity of the silk fabrics was assessed against *Staphylococcus aureus* (Gram-positive) and *Escherichia coli* (Gram-negative) according to the AATCC 100–2004 test method. Fabric swatches (5 × 5 cm) were inoculated with 0.4 mL of bacterial suspension containing approximately 3.6×10^6 CFU/mL in nutrient broth. Both control (undyed) and test samples were incubated with the bacterial inoculum for 24 h. After incubation, 100 mL of sterilised distilled water was added to each vessel and shaken vigorously. The supernatant was serially diluted and plated on nutrient agar, followed by incubation at 37 °C for 24 h. Viable bacterial colonies were counted, and the reduction in bacterial population (R, %) was calculated using the following equation:

$$R = (A-B)/A \times 100 \quad \ldots (2)$$

where *A* is the number of bacterial colonies on the control (undyed fabric); and *B*, number of colonies on the dyed fabric.

2.8 Laundering Durability of Antibacterial Activity

The durability of the antibacterial property after laundering was assessed using a Launder-O-Meter in accordance with AATCC 61–1994, where one cycle corresponded to five home laundering cycles. After laundering, the antibacterial activity of the fabrics was evaluated using the same procedure described above.

3 Results and Discussion

3.1 Characterisation of AgNPs

Figure 1 shows the colour of AgNP solutions synthesised using varying amounts of sodium borohydride ($NaBH_4$) as the reducing agent. As the volume of 0.1 M $NaBH_4$ solution increases from 6.0 to 8.0, 12.8, 16.0, 16.8, and 20.0% of the $AgNO_3$ solution, the colour of the colloidal dispersions changes sequentially from light blue to navy, violet, green, red, and yellow, respectively. These distinct colour variations arise from the localised surface plasmon resonance (LSPR) characteristics of the AgNPs. The optical properties, and consequently the colour, of metallic nanoparticles such as silver are known to depend on their size, shape, and surrounding dielectric environment[30]. Moreover, metals possessing free conduction electrons, including copper, silver, and gold, exhibit strong plasmon resonances within the visible range, giving rise to vivid colours[31].

The UV–Visible (UV–Vis) absorption spectra of the AgNPs with different colours (Fig. 2) confirm the

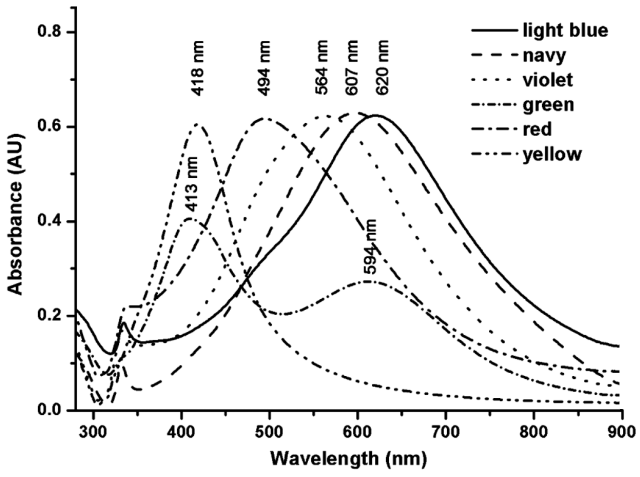

Fig. 2 — UV-vis absorption spectra of synthesised AgNPs exhibiting different colours

successful formation of nanoparticles via the reduction of Ag^+ ions. Five samples—light blue, navy, violet, red, and yellow—display single, well-defined absorption peaks at 620, 607, 564, 494, and 418 nm, respectively. These distinct peaks correspond to the dipole plasmon resonance of the AgNPs, suggesting the formation of uniform nanoparticle populations in each case. The green AgNP solution, however, exhibits two absorption bands at approximately 594 and 413 nm, which correspond to the resonances of blue and yellow AgNPs, respectively. This indicates the coexistence of two nanoparticle populations with different morphologies, giving rise to the observed green colour.

Transmission electron microscopy (TEM) provides detailed insights into the morphology and size distribution of the synthesised AgNPs (Fig. 3). The light blue, navy, and violet AgNPs predominantly appear as triangular nanoplates with varying aspect ratios [Fig. 3 (a) – (c)], whereas the red and yellow AgNPs exhibit nanodisk morphologies [Fig. 3 (e) & (f)]. The green AgNPs consist of a mixture of both triangular nanoplates and nanodisks (Fig. 3 (d)), confirming their heterogeneous nature. The average particle sizes for light blue, navy, violet, red, and yellow AgNPs are approximately 79.8, 44.9, 28.9, 7.0, and 2.8 nm, respectively, while the green AgNPs display a broader size distribution ranging from 3.8 to 39.5 nm. These morphological differences directly influence the LSPR characteristics of the nanoparticles, resulting in the distinct colour variations observed.

3.2 Characterisation of AgNPs Dyed Silk Fabrics

The LSPR characteristics of AgNPs enable the production of vividly coloured silk fabrics through an *in situ* dyeing process, eliminating the need for conventional dyes[32]. Photographs of the dyed silk fabrics (Fig. 4) reveal a wide colour range, achieved solely by varying the morphology and concentration of AgNPs. This demonstrates that nanoparticle geometry and size can effectively tune the optical appearance of fabrics.

To quantitatively evaluate colour variation, the colour strength (K/S) values of AgNP-dyed fabrics are measured across the wavelength range of 380–700 nm (Fig. 5). The navy-AgNP-dyed fabric exhibits the highest K/S value at approximately 590 nm. As the fabric colour shifts from light blue to other hues, the corresponding K/S peak gradually undergoes a blue shift, consistent with the observed LSPR changes in the AgNP solutions. The K/S curve for the green-AgNP-dyed fabric shows broad overlapping peaks, reflecting its composite nanoparticle population. These spectral shifts confirm that the LSPR of AgNPs governs the tunable colouration of the silk fabrics, and that the maximum K/S wavelength can be precisely adjusted by manipulating nanoparticle morphology.

Colorimetric analysis (Table 1) further supports these findings. The white control silk fabric exhibits a marked transformation in colour after dyeing with AgNPs, displaying light blue, navy, violet, green, red, and yellow hues depending on the AgNP morphology. The total colour difference (ΔE) values, calculated using CIE L*a*b* coordinates, are determined to be

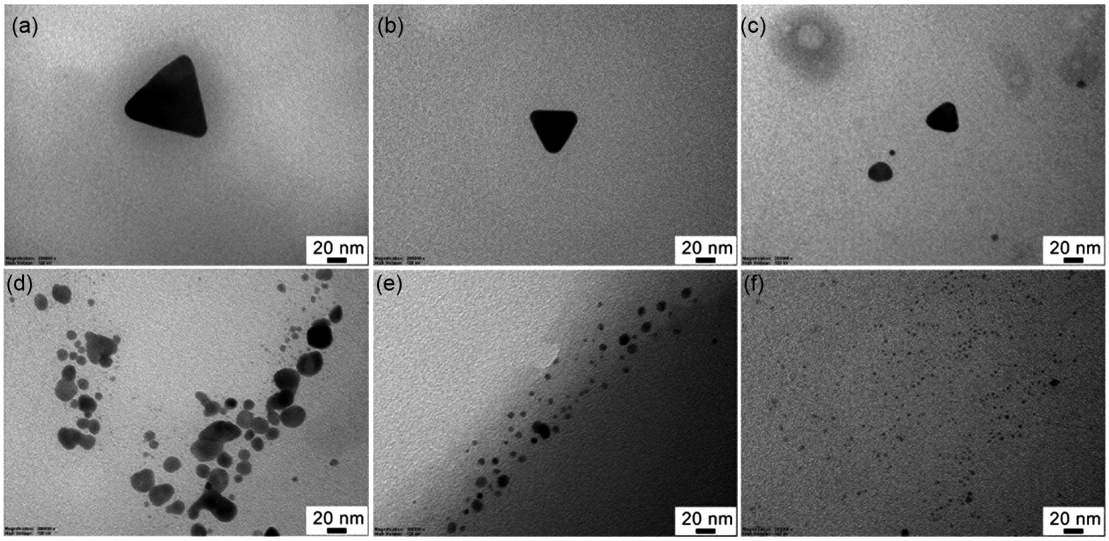

Fig. 3 — TEM images of synthesised AgNPs showing different colours (a) light blue, (b) navy, (c) violet, (d) green, (e) red, and (f) yellow

Table 1 — Colour coordinates and K/S values of undyed and AgNPs dyed silk fabrics

Sample fabric	L*	a*	b*	ΔE	K/S
Control	99.31	-0.07	0.14	-	-
Light blue-AgNPs dyed	74.82	7.11	-9.26	27.20	0.54
Navy-AgNPs dyed	64.54	6.10	-5.62	35.78	0.74
Violet-AgNPs dyed	66.02	5.13	-6.00	34.25	0.67
Green-AgNPs dyed	72.33	1.67	4.54	27.34	0.48
Red-AgNPs dyed	70.61	5.50	11.04	31.20	0.72
Yellow-AgNPs dyed	72.41	4.00	17.64	32.35	0.67

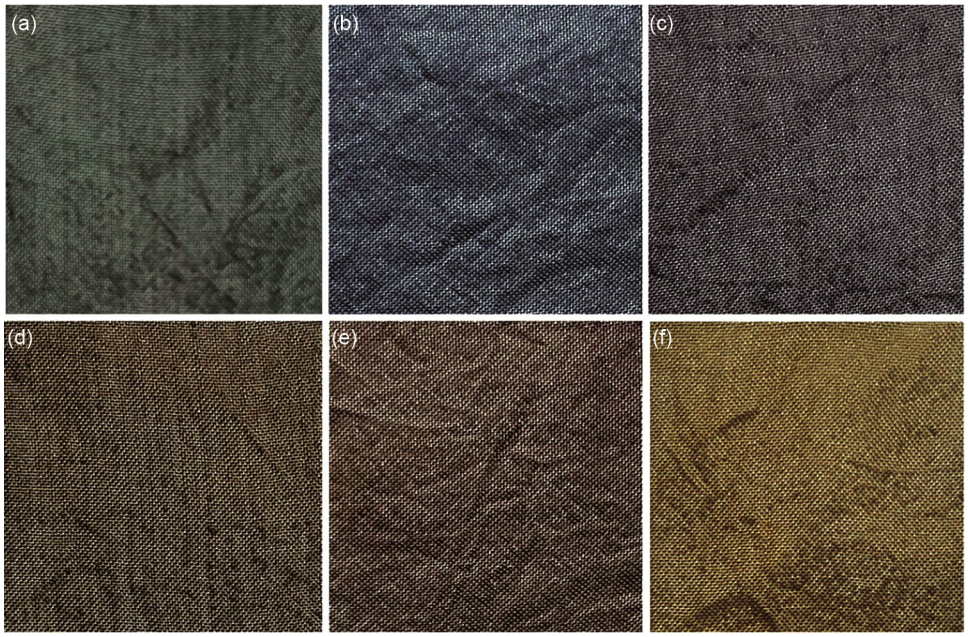

Fig. 4 — Photographs of silk fabrics dyed with synthesised AgNPs showing corresponding colours (a) light blue, (b) navy, (c) violet, (d) green, (e) red, and (f) yellow

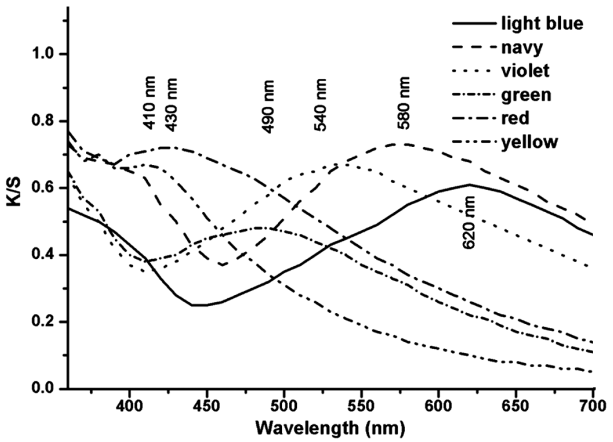

Fig. 5 — K/S curves of silk fabrics dyed with synthesised AgNPs

27.20, 35.78, 34.25, 27.34, 31.20, and 32.35 for light blue, navy, violet, green, red, and yellow dyed fabrics, respectively. All dyed samples reveal decreased L* values and increased a* values relative to the undyed fabric, indicating a darker and more saturated colouration. Furthermore, b* (yellowness) values are lower for blue- and violet-toned fabrics due to the bluish appearance conferred by the corresponding nanoparticles. Consistent with these observations, the K/S values increase from nearly zero in the undyed fabric to 0.54, 0.74, 0.67, 0.48, 0.72, and 0.67 for the light blue, navy, violet, green, red, and yellow samples, respectively, reflecting enhanced dye uptake and strong colour intensity consistent with optical data.

Scanning electron microscopy (SEM) images (Fig. 6) reveal distinct surface differences between undyed and AgNP-dyed silk fabrics. The neat silk fabric displays a smooth, uniform fibrous surface with regular fibre morphology [Fig. 6 (a)][33]. In contrast, the AgNP-dyed silk fabric [Fig. 6 (b)] exhibits visible nanoparticles deposited on the fibre surfaces, contributing to the fabric's enhanced colouration.

The physical and mechanical properties of the dyed fabrics are summarised in Table 2. A slight reduction

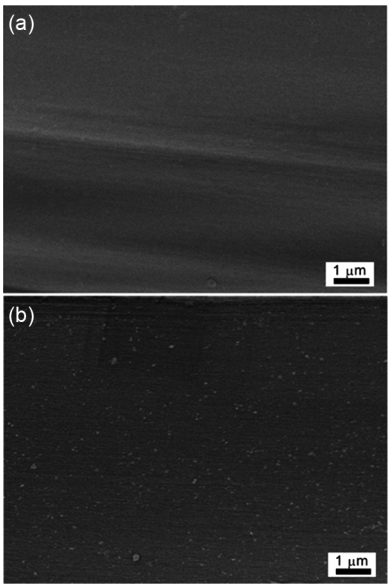

Fig. 6 — SEM images of (a) control, and (b) AgNPs-dyed silk fabric

Table 2 — Physical and mechanical properties of undyed and AgNPs dyed silk fabrics

Property	Control	AgNPs dyed
Fabric mass, g/m^2	73.2±0.206	74.2±0.165
Fabric thickness, mm	0.05±0.004	0.05±0.016
Tensile strength, N/mm^2	174.4±0.309	167.1±0.021
Elongation, %	13.2±0.761	12.3±0.735

in tensile strength and elongation is observed for AgNP-dyed silk compared with the control sample. Although silk fibres possess excellent acid resistance[34], the mild acidity of the AgNP dye bath and thermal exposure during the process can slightly weaken peptide linkages within the fibroin structure. Nevertheless, the overall mechanical integrity of the fabric remains largely preserved, indicating that the dyeing process has minimal adverse effects on fibre performance.

3.3 Antibacterial Activity

Beyond imparting colour, incorporating AgNPs confers significant antibacterial functionality to the silk fabrics. The antimicrobial activity is assessed against *S. aureus* and *E. coli*. Figure 7 shows that the agar plates containing undyed silk display dense bacterial colonies, confirming the absence of antibacterial properties. In contrast, the plates with AgNP-dyed silk exhibit markedly fewer colonies, indicating strong antibacterial efficacy.

Quantitative analysis of bacterial reduction (Table 3) reveals that the AgNP-dyed silk fabric achieves bacterial reductions of 99.9 % against

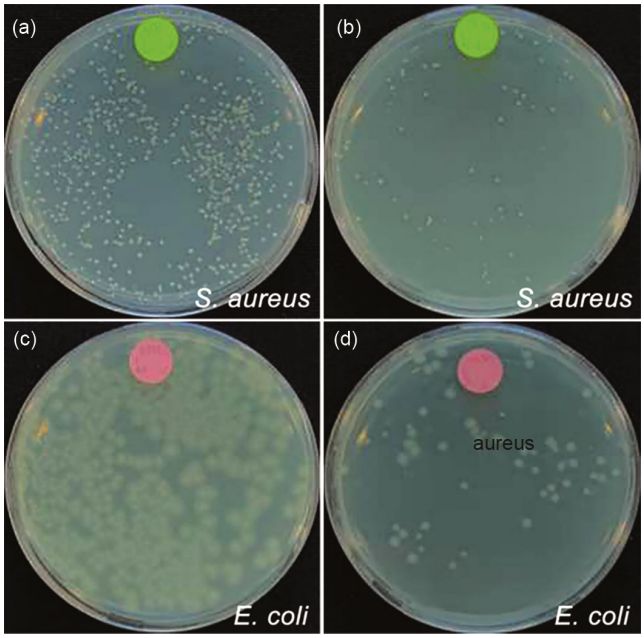

Fig. 7 — Antibacterial activity of (a, c) control, and (b, d) AgNPs-dyed silk fabrics against *S. aureus* and *E. coli*

Table 3 — Percentage bacterial reduction of silk fabrics dyed with AgNPs before and after washing cycles

Microbe	Sample	Bacterial reduction, %		
		0 cycle	5 cycles	10 cycles
S. aureus	Control	-	-	-
E. coli	AgNPs dyed silk fabric	99.9	99.2	98.9
	Control	-	-	-
	AgNPs dyed silk fabric	91.7	90.9	90.1

S. aureus and 91.7 % against *E. coli* after 24 h of incubation. These reductions exceed the 90 % threshold typically indicative of effective antibacterial performance. The observed activity is consistent with earlier reports on silver nanoparticle-treated natural fibres such as wool, where the release of Ag^+ ions disrupts bacterial membranes and inhibits metabolic processes[35-37].

The antibacterial durability of the AgNP-dyed silk is further evaluated through repeated laundering. Even after ten washing cycles, the fabrics retain 98.9 % and 90.1 % bacterial reduction against *S. aureus* and *E. coli*, respectively. This excellent durability is attributed to the strong electrostatic interaction between negatively charged AgNPs and the cationised silk surface pretreated with CHTAC. CHTAC, a cationic modifying agent, has been adsorbed by silk to promote cationic silk fabric[38]. The tight binding between the nanoparticles and the fabric matrix ensures minimal leaching of silver during washing, maintaining both antibacterial efficiency and colour stability.

4 Conclusion

This study demonstrates that silver nanoparticles (AgNPs) with tunable morphologies can impart vivid and durable colours to silk fabrics while simultaneously providing strong antibacterial functionality. The distinct hues obtained arise from the localised surface plasmon resonance characteristics of AgNPs, which can be precisely controlled by varying the reducing agent concentration during synthesis. The dyed fabrics exhibit uniform nanoparticle deposition, high colour strength, and minimal loss of mechanical integrity. Moreover, the AgNP-treated silk shows excellent antibacterial activity against *Staphylococcus aureus* and *Escherichia coli*, retaining over 90% efficacy even after multiple washes. The process operates efficiently at room temperature within a short duration, offering a promising, energy-efficient colouration method for the textile industry, combining aesthetic appeal with functional benefits.

References

1 Nilesh I & Warren J J, *Text Res J*, 95 (2025) 625.
2 Attia N F, Ahmed H E, El Ebissy A A & El Ashery S E A, *Prog Org Coat*, 166 (2022) 106822.
3 Ehsanimehr S, Sonnier R, Najafi P, Ducos F, Badawi M, Formela K, Saeb M R & Vahabi H, *React Funct Polym*, 173 (2022) 105221.
4 Taheri P & Khajeh-Amiri A, *Macromolecules*, 158 (2020) 282.
5 Li Q, Zhang S, Mahmood K, Jin Y, Huang C, Huang Z, Zhang S & Ming W, *Prog Org Coat*, 157 (2021) 06296.
6 Siddig E A A, Zhang Y, Yang B, Wang T, Shi J, Guo Y, Xu Y & Zhang J, *Mater Lett*, 308 (2022) 131189.
7 Zhenjie W, Yuwei G, Xiyu S, Chuliang S, Yijun J, Ruyi X, *Int J Biol Macromol*, 289 (2025) 138684.
8 Esfandiar P, Suju F, Jianming C & Xungai W, *Appl Surf Sci Adv*, 29 (2025) 100814.
9 Nitayaphat W, P Jirawongcharoen & Trijaturon T, *J Nat Fibers*, 15 (2018) 262
10 Roy S, Zhai L, Kim J W, Kim H C & J Kim *Prog Org Coat*, 140 (2020) 105500.
11 Thite A G, Krishnanand K, Sharma D K & Mukhopadhyay A K, *Radiat Phys Chem*, 153 (2018) 173.
12 Maghimaa M & Alharbi S A, *J Photochem Photobiol B*, 204 (2020) 111806.
13 Abdelghaffar F, Mahmoud M G, Asker M S & Mohamed S S, *J Ind Eng Chem*, 99 (2021) 224.
14 Gao Y N, Wang Y, Yue T-N, Weng Y-X & Wang X, *J Colloid Interface Sci*, 582 (2021) 112.
15 Petryayeva E & Krull U J, *Anal Chim Acta*, 706 (2011): 8-24.
16 Wu C, Zhou X & Wei J, *Nanoscale Res Lett*, 10 (2018) 354.
17 Kelly K L, Coronado E, Zhao L L & Schatz G C, *J Phys Chem B*, 107 (2003) 668677.
18 Sherry L J, Jin R C, Mirkin C A, Schatz G C & Van Duyne R P, *Nano Lett*, 6 (2006) 2060.
19 Ilic´ V, Šaponjic´ Z, Vodnik V, Potkonjak B, Jovancˇic´ P, Nedeljkovic´ J & Radetic´ M, *Carbohydr Polym*, 78 (2009) 564.
20 Loiseau A, Asila V, Boitel-Aullen G, Lam M, Salmain M & Boujday S, *Biosensors Basel*), 9 (2019) 78.
21 Mahamud S, Pervez N, Taher M A, Mohiuddin K & Liu H-H, *Text Res J*, 90 (2019) 1224.
22 Hasan K M F, Wang H, Mahmud S, Jahid M A, Islam M, Jin W & Genyang C, *J Mater Res Technol*, 9 (2020) 16135.
23 Lu Z, Mao C, Meng M, Liu S, Tian Y, Yu L, Sun B & Li C M, *J Colloid Interface Sci*, 435 (2014) 8.
24 Shubha P, LikhithGowda M, Namratha K, Shyamsunder S, Manjunatha H B & Byrappa K, *Mater Chem Phys*, 231 (2019) 21.
25 Tang B, Wang J, Xu S, Afrin T, Xu W, Sun L & Wang X, *J Colloid Interface Sci*, 356 (2011) 513.
26 Tang B, Sun L, Kaur J, Yu Y & Wang X, *Dyes Pigm*, 103 (2014) 183.
27 Metraux G S & Mirkin C A, *Adv Mater*, 17 (2005) 412.
28 Marwa A A, Khaled M S, Ahmed G H & Nancy S E, *Sci Rep*, 15 (2025) 14743.
29 Ruoying Z, Yingwei C, Leixu C, Guigang S, Zhengyuan H, Miaomiao X, Xiaotong W, Jixian G, Zaisheng C & Shixiong Z, *Cellulose*, 32 (2025) 2055.
30 Nasrollahzadeh M, Atarod M, Sajjadi M, Sajadi S M &, Issaabadi Z, *Interface Sci Technol*, 28 (2019) 199.
31 Khan I, Saeed K & Khan I, *Arab J Chem*, 12 (2019) 908.
32 Hassan M M, *Colloids Surf A Physicochem Eng Asp*, 581 (2019) 123819.
33 Zhang Z, Lv X, Chen Q & An J, *J Eng Fibers Fabr*, 14 (2019) 1.
34 Jiaojiao L, Ran C, Zhi L, Jing C, Qingmeng X & Junchang Y, *Archaeol Anthropol Sci*, 17 (2025) 68
35 Tiantian C, Yan Z, Jun Z & Bing Z, *Cellulose*, 32 (2025) 613.
36 Boroumand M N, Montazer M, Simon F, Liesiene J, Šaponjic Z & Dutschk V, *Appl Surf Sci*, 346 (2015) 477.
37 Hasan K M F, Pervez M N, Talukder M E, Sultana M Z, Mahmud S, Meraz M M, Bansal V & Genyang C A, *Nanomaterial*s, 9 (2019) 569.
38 Nitayaphat W & Jintakosol T, *Asian J Chem*, 32 (2020), 2275.